Physics Letters A 417 (2021) 127681

Contents lists available at ScienceDirect

Physics Letters A

www.elsevier.com/locate/pla

Gyrokinetic simulations of double tearing modes in toroidal plasma

Y. Yao [a], Zhihong Lin [b], J.Q. Dong [c], P. Shi [c], S.F. Liu [a], Jingchun Li [d,*]

[a] School of Physics, Nankai University, Tianjin 300071, People's Republic of China
[b] University of California, Irvine, CA 92697, USA
[c] Southwestern Institute of Physics, Chengdu 610041, People's Republic of China
[d] Department of Earth and Space Sciences, Southern University of Science and Technology, Shenzhen 518000, People's Republic of China

ARTICLE INFO

Article history:
Received 11 July 2021
Received in revised form 11 August 2021
Accepted 10 September 2021
Available online 15 September 2021
Communicated by A. Das

Keywords:
Double tearing mode
Magnetic island
Gyrokinetics
Numerical modeling

ABSTRACT

An investigation of the characteristics of double-tearing modes (DTMs) and the influence of the kinetic effects of ions has been carried out with the gyrokinetic code GTC. A simplified linear fluid and a gyrokinetic model has been used for the electron and ion dynamics, respectively. It was found that as the separation of the rational surfaces was increased, the growth rates of DTMs were enhanced and the DTM system tended to decouple into a system of two single-tearing modes. When the width between the rational surfaces is larger, the corresponding amplitude of the inner-tearing mode is smaller. We also demonstrate that the existence of thermal ions destabilizes the DTM. The toroidal effect also has a mild destabilizing effect ($\sim 8\%$) on the growth of DTMs, which is consistent with the theoretical analysis.

1. Introduction

Tearing modes (TMs) are macro-instabilities driven by the plasma current. The advanced tokamak configuration requires that q has a reversed shear, which results in the appearance of double-tearing modes (DTMs). The DTM's instability due to the negative magnetic shear, s, is very important in fusion plasma because it leads to low plasma confinement and even plasma disruption [1–10]. Therefore, studying the characteristics of DTMs is essential for the steady-state operation of future tokamaks. Additionally, the study of TMs can strengthen the understanding of the phenomenon of magnetic reconnection in astrophysics [11,12].

In their previous work, Furth et al. presented the scaling rate of the growth rate of the linear single TM with respect to resistivity as $\eta^{3/5}$ under the approximation of constant ψ and $\eta^{1/3}$ assuming non-constant ψ [13]. Ofman and Chen et al. gave its linear growth rate with respect to resistivity and viscosity as $\eta^{5/6}\mu^{-1/6}$ [14,15]. Einaudi and Rubini [16] studied the effect of kinematic viscosity on the characteristics of resistive TMs. They found that the viscosity could have both a damping or destabilizing effect, depending on the ratio between the viscosity and the Alfven velocity. P. L. Pritchett investigated the TM within the framework of magnetohydrodynamics. With increasing width between the rational surfaces, the mode has a scaling (of the magnetic Reynolds number S) of $S^{-3/5}$ and its structure resembles a standard TM [16].

There have been many theoretical and numerical investigations focused on DTMs [17–20]. Dong et al. studied the DTMs induced by anomalous electron viscosity [18–21], and found that the scaling relationship of their linear growth rate changes from $S^{-1/5}$ to $S^{-1/3}$ as the distance between rational planes increases. Zhang et al. considered the Hall effect and numerically studied the growth rate of the double tearing mode during the dramatic growth phase in Hall MHD simulation [22]. Recently, X. Q. Wang studied the DTMs in plasmas with rotations, and found that differential plasma rotation has a remarkable stabilizing influence on the DTMs [23]. Recently, the effects of asymmetric magnetic perturbation [24], shear flows [25], electron cyclotron current drive (ECCD) [26], plasma flow [27], and plasmoids [28] on the nonlinear evolution of DTMs have also been investigated.

Most of the above-mentioned research on the resistive DTMs was restricted to the cylindrical configuration. Studies on the DTMs of plasma in the toroidal configuration are not adequate. In addition, the influence of the kinetic effect on the DTM is not clear. In this work, we used the method of gyrokinetics to study the toroidal and kinetic effects on the linear instability of the DTMs. We found that as the rational surface's width is increased, the growth rates of DTM are enhanced, and the double-tearing mode system tends to decouple into two single-tearing modes. The existence of thermal ions destabilizes the DTM, while the toroidal effect could slightly destabilize the DTMs.

* Corresponding author.
E-mail address: jingchunli@pku.edu.cn (J. Li).

https://doi.org/10.1016/j.physleta.2021.127681
0375-9601/

The paper is organized as follows: In Sec. 2, a gyrokinetic model of tearing mode is presented. The simulation parameters are derived in Sec. 3. A description of our results is presented in Sec. 4. We discuss our results briefly in Sec. 5.

2. Model

An inertialess electron fluid model, coupling with the gyrokinetic ions through Ampere's law and the gyrokinetic Poisson's equation, can be utilized to study the double-tearing mode instability [29–33].

We start from the gyro-kinetic equation:

$$\frac{\mathrm{d}}{\mathrm{d}t} f_\alpha(\boldsymbol{X}, \mu, v_\parallel, t) = (\frac{\partial}{\partial t} + \dot{\boldsymbol{X}}\cdot\nabla + \dot{v}_\parallel \frac{\partial}{\partial v_\parallel}) f_\alpha = (\frac{\partial}{\partial t} f_\alpha)_{collision} \quad (1)$$

where:

$$\dot{\boldsymbol{X}} = v_\parallel \frac{\boldsymbol{B}}{B_0} + \frac{c\boldsymbol{b_0}\times\nabla\phi}{B_0} + \frac{v_\parallel^2}{\Omega_\alpha}\nabla\times\boldsymbol{b_0} + \frac{\mu}{m_\alpha\Omega_\alpha}\boldsymbol{b_0}\times\nabla B_0 \quad (2)$$

$$\dot{v}_\parallel = -\frac{1}{m_\alpha}\frac{\boldsymbol{B^*}}{B_\parallel^*}\cdot(\mu\nabla B_0 + Z_i\nabla\phi) - \frac{Z_\alpha}{m_\alpha c}\frac{\partial A_\parallel}{\partial t} \quad (3)$$

Here, $\boldsymbol{X}$, μ, and $v_\parallel$ represent the particle guiding center position, the magnetic moment, and the parallel velocity. A pitch-angle scattering collision operator is used for the resistivity, where f_{e0} is the equilibrium distribution function. m_α and Ω_α are respectively the particle mass and cyclotron frequency, and the formula of $\boldsymbol{B^*}$ can be seen in Ref. [34]. We derived the perturbed fluid continuity equation of electrons from Eq. (1):

$$\begin{aligned}
&\frac{\partial}{\partial t}\delta n_e + \boldsymbol{B_0}\cdot\nabla(\frac{n_{e0}\delta u_{\parallel e}}{B_0}) + B_0\delta\boldsymbol{v_E}\cdot\nabla(\frac{n_e}{B_0}) \\
&-n_{e0}(\delta\boldsymbol{v_{*e}} + \delta\boldsymbol{v_E})\cdot\frac{\nabla B_0}{B_0} + \delta\boldsymbol{B}\cdot\nabla(\frac{n_{e0}u_{\parallel e0}}{B_0}) \\
+\frac{c\nabla\times\boldsymbol{B}_0}{B_0^2}\cdot(&-\frac{\nabla\delta p_e}{e} + n_{e0}\nabla\delta\phi) + \{\delta\boldsymbol{B}\cdot\nabla(\frac{n_{e0}\delta u_{\parallel e}}{B_0}) \\
&+B_0\delta\boldsymbol{v_E}\cdot\nabla(\frac{\delta n_e}{B_0}) + \frac{c\nabla\times\boldsymbol{B_0}}{B_0^2}\cdot\delta n_e\nabla\delta\phi\}_{NL} = 0
\end{aligned} \quad (4)$$

The equation of parallel momentum can also be written as:

$$\begin{aligned}
&n_{e0}m_e\frac{\partial}{\partial t}\delta u_{\parallel e} + n_{e0}m_e\boldsymbol{u_{\parallel e0}}\cdot\nabla\delta u_{\parallel e} = \\
&\qquad -n_{e0}e(-\nabla_\parallel\delta\phi - \frac{1}{c}\frac{\partial\delta A_\parallel}{\partial t}) \\
&-\frac{\delta\boldsymbol{B}}{B_0}\cdot\nabla p_{e0} - \nabla_\parallel\delta p_e - n_{e0}m_e\nu_{ei}\delta u_{\parallel e}
\end{aligned}$$

where $v_E = \frac{c\boldsymbol{b_0}\times\nabla\phi}{B_0}$ is the drift velocity and is gyro-center averaged. $\delta v_{*e} = \frac{1}{n_0 m_e\Omega_e}\boldsymbol{b_0}\times\nabla(\delta p_\parallel + \delta p_\perp)$, $\delta p_e = \delta n_e T_e + \delta\boldsymbol{r}\cdot\nabla(n_{e0}T_e)$, and $\delta\boldsymbol{r}$ is the displacement of the fluid elements. The sub-index "NL" means the nonlinear term. $n_e = n_{e0} + \delta n_e$, $\delta\phi$, $\delta A_\parallel$ are the perturbed electrostatic potential and perturbed parallel vector potential, respectively. We drop the electron inertial term here. Thus, we get the parallel force balance equation through the inertialess electron momentum equation:

$$\frac{\partial\delta A_\parallel}{\partial t} = -c\boldsymbol{b_0}\cdot\nabla\delta\phi + \frac{c}{n_{e0}e}\boldsymbol{b_0}\cdot\nabla\delta p_e - c\eta\delta j \quad (5)$$

where $\delta j = -\frac{c}{4\pi}\nabla_\perp^2\delta A_\parallel$, $\eta = m_e\mu_{ei}/e$ is the resistivity, $\delta\boldsymbol{B} = \nabla\times\delta A_\parallel b_0$, n is the toroidal mode number, and m is the poloidal mode number. Neglecting the nonlinear term, and considering a uniform equilibrium pressure, Eq. (4) can be simplified as:

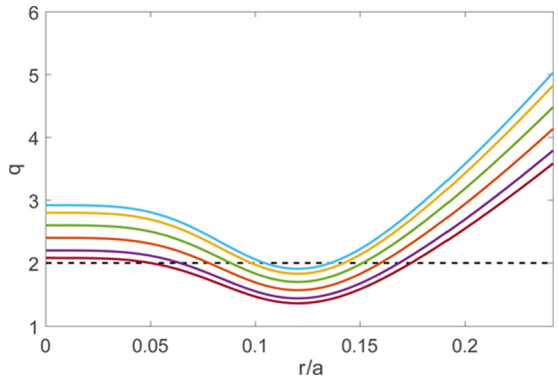

Fig. 1. q profile used in the simulations with different D_{12} respectively. The different q profiles here are obtained by changing the parameter q_c in Eq. (9).

$$\frac{\partial}{\partial t}\delta n_e = -\boldsymbol{B_0}\cdot\nabla(\frac{n_{e0}\delta u_{\parallel e}}{B_0}) - \boldsymbol{\delta B}\cdot\nabla(\frac{n_{e0}u_{\parallel e0}}{B_0}) \quad (6)$$

Here, we assume the electrons are isothermal along perturbed magnetic field line, i.e., $T_e =$ constant, $p_e = n_e T_e$, to close the fluid model, with the gyrokinetic Poisson's equation

$$\frac{4\pi Z_i^2}{T_i}(\delta\phi - \delta\tilde{\phi}) = 4\pi(Z_i\delta n_i - e\delta n_e) \quad (7)$$

and the parallel Ampere's law

$$en_{e0}\delta u_{\parallel e} = \delta j + Z_i n_{i0}\delta u_{\parallel i}. \quad (8)$$

The parameters n_i and $u_{\parallel i}$ can be obtained from the standard gyrokinetic model for ions [29,30], that is from the Eqs. (1)-(3) with $\alpha = i$. The coupling of the gyrokinetic ions from Eq. (5) and the fluid electrons from Eq. (6) is described by equations (7) and (8). These equations provide a closed system for study of the low-frequency magnetohydrodynamic instabilities.

3. Simulation setup

With solving the Eqs. (1)-(3) and Eqs. (5)-(8), we could investigate the DTMs. Now we utilize this model to investigate the evolution of DTMs and the influence of kinetic ions and toroidal geometry. The simulation parameters are: inverse aspect ratio $\epsilon = a/R_0 = 0.242$, major radius $R_0 = 165$ cm, magnetic field $B_0 = 12700$ G, the equilibrium electron density on magnetic axis $n_{e0} = 10^{14}/\mathrm{cm}^3$, the plasma temperature $T_i = T_e = 4500$ eV, the resistivity $\eta = 9\times10^{-6}\ \Omega\cdot$m. The resistivity is fixed in our simulations and our preliminary results show that the growth rate of DTM is $\eta^{1/5}$ dependent.

The q profile we used has the form

$$q(r) = q_c\{1 + (\frac{r}{r_0})^{2\lambda}\}[1 + Aexp\{-(\frac{r - r_\delta}{\delta})^2\}] \quad (9)$$

For the (2,1) DTM, the parameters were set as $\lambda = 1$, $r_0 = 0.412$, $\delta = 0.273$, $r_\delta = 0$, $A = 3$, q_c=0.6, the positions of $q = 2$ flux surfaces, and the separation between the two rational surfaces D_{12} was varied.

The q profiles used in the simulations with different D_{12} are shown in Fig. 1. By modifying the parameters, different safety factor profiles can be simulated. The width and position of the magnetic island can be modified by changing the parameter q_c.

4. Simulation results

We first give a typical double-tearing mode fluid/gyrokinetic simulation result in Fig. 2, given the mode structures of (m/n) = (2, 1) DTMs on the poloidal plane and its radial profile. Fig. 2(a)

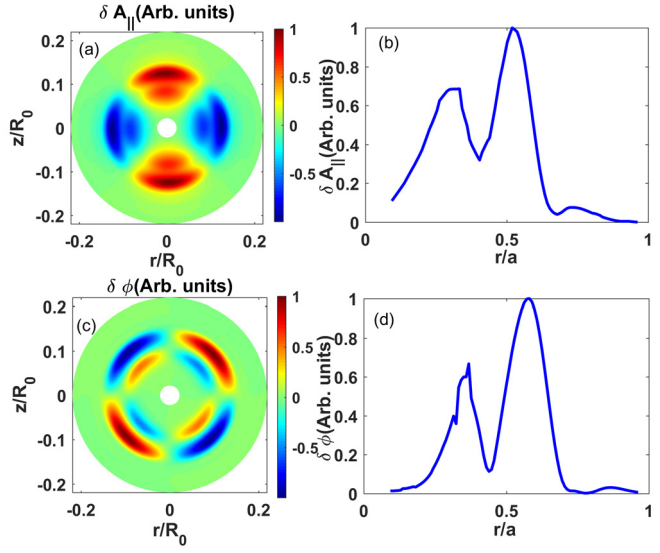

Fig. 2. $(m/n) = (2, 1)$ DTMs mode structure. (a) and (c) are the contours of $\delta A_\parallel$ and $\delta\phi$ on the 2D poloidal cross-section. (b) and (d) are the radial profile of $\delta A_\parallel$ and $\delta\phi$ at $\theta = 90°$ and $\theta = 45°$, respectively.

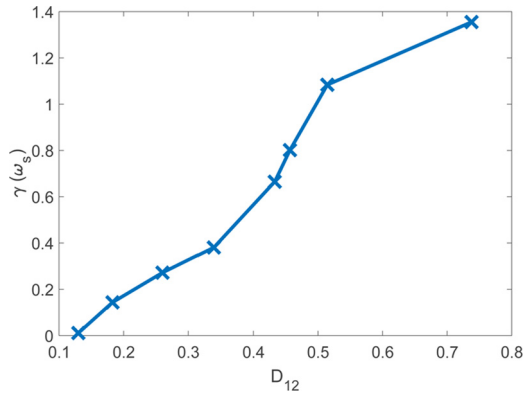

Fig. 3. The growth rate of DTMs versus rational surfaces width.

and (c) are the contours of $\delta A_\parallel$ and $\delta\phi$ in the 2D poloidal cross-section, respectively. Fig. 2(b) and (d) are the radial distributions of $\delta A_\parallel$ and $\delta\phi$ at $\theta = 90°$ and $\theta = 45°$, respectively, for $D_{12} = 0.18$. The case in Fig. 2 corresponds to $D_{12} = 0.18$. All results in the figure are normalized to their maximum values. In our calculations we retained only the (2,1) mode; the other modes are filtered out via Fourier transformation. It can be seen that the mode structure presents a typical (2,1) double TMs structure. The strength and width on the inner side of the DTMs are smaller than on the outer side, which can also be seen from the radial profile.

We next studied the relationship between the characteristics of the double TMs and the distance between the two rational surfaces. Fig. 3 shows the normalized growth rate of DTMs versus the normalized distance between the two rational surfaces D_{12}. It is evident that growth rate increases almost linearly with the distance, indicating that the greater the separation between the two rational surfaces, the greater the growth rates of DTMs.

The influence of the width of separation of the rational surfaces on the poloidal contour plots of $\delta\phi$ and $\delta A_\parallel$ is given in Fig. 4. When the separation between the rational surfaces is large ($D_{12} \geq 0.61$), the potential perturbation and magnetic vector potential perturbation only appear near the outer rational surface. When the rational surfaces' separation is small enough ($D_{12} \leq 0.26$), the perturbations appear on both rational surfaces. Comparing (a) with (c) (or (d) with (f)), it is clear that small rational surface separation results in a smaller radial width of the outer perturbation. When the distance between the two rational surfaces approaches a critical value, the magnetic islands on the two isolated rational surfaces will be coupled, and the magnetic island structure exhibits the characteristics of a double-tearing mode. The DTMs system decouples into a system of two single standard tearing modes when the distance between the rational surfaces increases sufficiently. In particular, when D_{12} is too large, one even cannot see the structure of inner instability mode. Thus, fluid/gyrokinetic calculations are qualitatively consistent with the previous fluid simulation results [14].

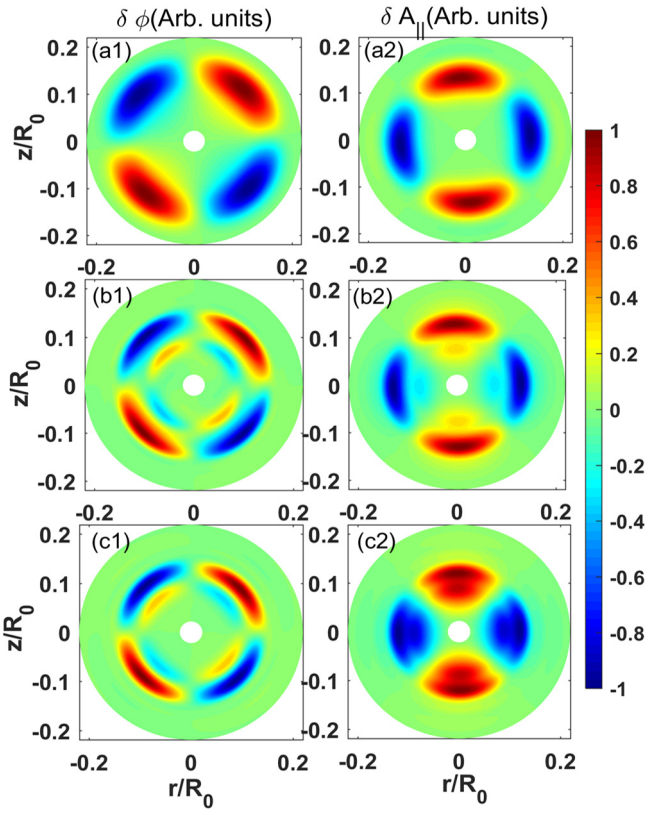

Fig. 4. Poloidal contour plots of $\delta\phi$ ((a1)(b1)(c1)) and $\delta A_\parallel$ ((a2)(b2)(c2)) with different separations of rational surfaces at step=3600. (a1)(a2): D_{12}=0.61, (b1)(b2): D_{12}=0.26, (c1)(c2): D_{12}=0.13.

The radial distributions of perturbed vector potentials corresponding to Fig. 4 are shown in Fig. 5. The peak wave amplitudes exist at the maximum of the $\delta\phi$ gradient in the outer region, the same as we found in our former single-tearing mode study [4]. Additionally, the corresponding amplitude of the inner tearing mode is smaller when D_{12} is large and therefore the peak of the wave is difficult to see, which is consistent with Fig. 4. In general, increasing D_{12} could increase the growth rate of TMs, but it will weaken the double-tearing mode characteristics of the magnetic island. When D_{12} is too large, the peak value of the inner mode structure ($\delta A_\parallel$) cannot be seen. This is because when D_{12} is too large, the instability exhibits the characteristics of two single TMs with significantly different growth rates. At the time the outer magnetic island reaches a larger size, the inner magnetic island structure has not yet completely risen, so we can only clearly see a single-tearing mode structure.

We next investigated the kinetic effect of thermal ions on the double TMs. Fig. 6 presents the growth rate of the DTMs versus separation of rational surfaces width with and without thermal ions. It shows that the existence of thermal ions has a destabilizing effect on the DTMs. Previous studies have shown that the effects of

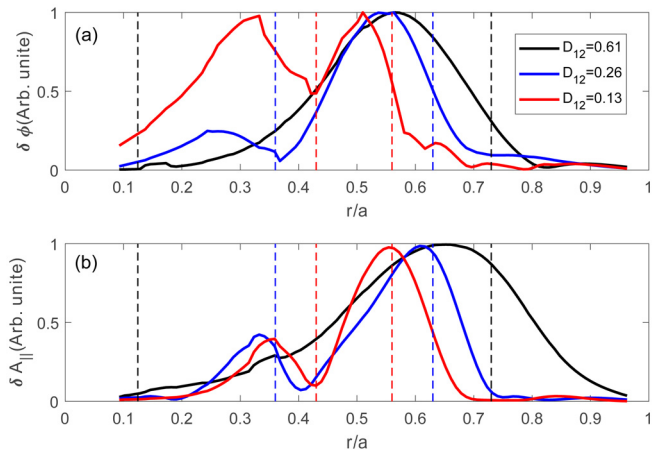

Fig. 5. Corresponding to Fig. 4, radial profile of the $\delta\phi$ (a) and $\delta A_{\parallel}$ (b) with three different D_{12} values at $\theta = 45°$ and $\theta = 90°$, respectively. The vertical dashed lines in the two panels show the location of the rational surface.

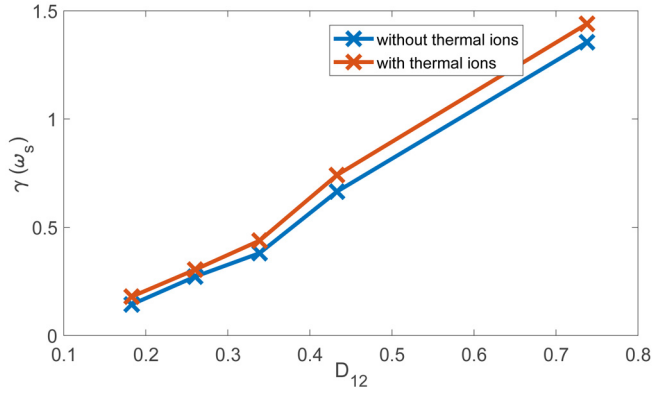

Fig. 6. The growth rate of DTMs versus separation of rational surfaces with thermal and without thermal ions.

kinetic ions are mainly introduced through the finite Larmor radius effect (FLR), Landau damping, ion acoustic waves (IAW) excitation, and the ion pressure gradient effect [35,36]. The first three have a stabilizing effect on instability, while the last has a destabilizing effect on instability. Regarding the influence of the ion thermal effect on the double-tearing mode, our results indicate that the ion pressure gradient driving is stronger than the ion Landau and FLR damping, while the generation of ion acoustic waves was not found in the simulation. Generally, under our simulation parameters, the existence of thermal ions destabilizes the DTMs.

Finally, we have studied the toroidal effect on the growth rate of DTMs with different separation of rational surfaces. The main difference between the toroidal and cylindrical configurations is the correction of the toroidal magnetic field. As considering toroidal configuration, the toroidal magnetic field is expressed as:

$$B_\zeta = \left[1 - \frac{r}{R_0}\cos\theta + \left(\frac{r}{R_0}\right)^2 \cos^2\theta\right] B_{\zeta 0} \tag{10}$$

The second-order correction term of the toroidal magnetic field is retained in the toroidal configuration. The second-order correction term can increase the radial shear of B_ζ. Since q is fixed in the simulation, the toroidal effect correspondingly increases the shear of the magnetic field in the poloidal direction, which provides the free energy for driving DTMs. Therefore, theoretically, the introduction of the toroidal effect can provide a larger driving force for DTMs. Fig. 7 demonstrates the growth rate of the DTM versus separation of rational surfaces in both cylindrical and toroidal configurations. This demonstrates that addition of the toroidal effect increases the growth rate of the DTM for different D_{12}, which is consistent with the previous theoretical analysis. The growth rate of the DTMs also increases with the increase of D_{12}, as shown in Fig. 3.

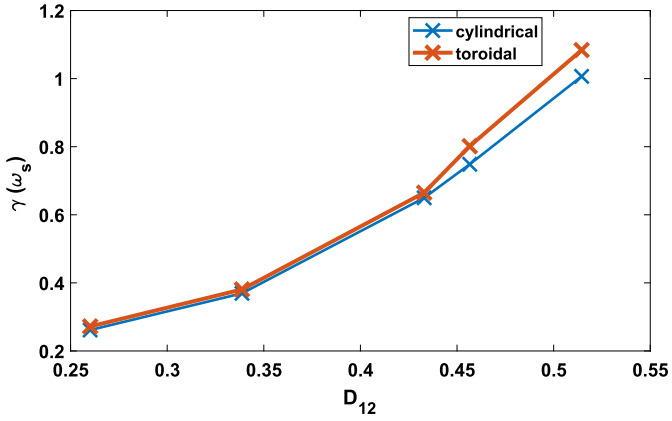

Fig. 7. The growth rate of DTMs versus separation of rational surfaces under cylindrical and toroidal configuration.

5. Conclusion

To summarize, using a fluid model for electrons and a gyrokinetic method for ions, the evolution of DTMs and the influence of kinetic effects on it has been investigated. It is found that with increasing the separation of the rational surfaces, the growth rates of DTMs enhance, and the mode tends to decouple into two single tearing modes. The existence of thermal ions destabilizes the mode, indicating that the ion pressure gradient driving is dominant when considering the effect of kinetic ions. The toroidal effect also enhances the growth of DTMs, which is consistent with the theoretical analysis. The basic characteristics of DTMs in the framework of gyrokinetics have been demonstrated. The future challenge lies in the description of nonlinear evolution of the DTMs with gyrokinetics and the influence of energetic particles taking into account.

CRediT authorship contribution statement

Y. Yao: Conceptualization, Methodology, Writing original draft preparation.
Zhihong Lin: Method design, Result analysis, Software.
J.Q. Dong: Methodology, Writing.
P. Shi: Methodology.
S.F. Liu: Investigation, Writing.
Jingchun Li: Supervision, Result analysis, Writing – review & editing.

Declaration of competing interest

The authors declare that they have no known competing financial interests or personal relationships that could have appeared to influence the work reported in this paper.

Acknowledgement

This work is supported by the National Key *R*&*D* Program of China (Nos. 2018YFE0303102 and 2017YFE0301702), the National Natural Science Foundation of China (Nos. 11905109 and 11947238), and the Center for Computational Science and Engineering of Southern University of Science and Technology. J. C. Li also thanks Y. Liu at NKU, W. Zhong, and J. Q. Xu at SWIP for fruitful discussions.

References

[1] Q. Yu, et al., Nucl. Fusion 39 (1999) 487.
[2] O. Sauter, et al., Phys. Plasmas 4 (1997) 1654.
[3] Y. Ishii, et al., Phys. Plasmas 7 (2000) 4477.
[4] Jingchun Li, et al., Phys. Plasmas 27 (2020) 042507.
[5] N. Arcis, et al., Phys. Lett. A 372 (2008) 5807.
[6] Z.X. Wang, et al., Nucl. Fusion 55 (2015) 043005.
[7] Z.X. Wang, et al., Phys. Rev. Lett. 99 (2007) 185004.
[8] K. Ida, et al., Phys. Rev. Lett. 88 (1) (2002) 015002.
[9] D. Li, et al., Chin. Phys. Lett. 10 (1998) 154.
[10] H. Cai, et al., Phys. Rev. Lett. 106 (2011) 075002.
[11] X.Y. Wang, et al., Phys. Plasmas 18 (2011) 122102.
[12] Y. Lin, et al., Plasma Phys. Control. Fusion 53 (2011) 054013.
[13] H.P. Furth, et al., Phys. Fluids 6 (1963) 459.
[14] L. Ofman, et al., Phys. Fluids B 3 (1991) 1364.
[15] X.L. Chen, et al., Phys. Fluids B 2 (1990) 2575.
[16] G. Einaudi, et al., Phys. Fluids B 1 (1989) 2224.
[17] P.L. Pritchett, et al., Phys. Fluids 23 (1980) 1368.
[18] J.Q. Dong, et al., Phys. Plasmas 10 (2003) 3151.
[19] J.Q. Dong, et al., Phys. Plasmas 11 (2004) 5673.
[20] Z.X. He, et al., Phys. Plasmas 17 (2010) 112102.
[21] Z.X. He, et al., Phys. Scr. 82 (2010) 065507.
[22] C.L. Zhang, et al., Phys. Plasmas 16 (2009) 122113.
[23] X.Q. Wang, et al., Phys. Plasmas 18 (1) (2011) 1951.
[24] G.Z. Xiong, et al., Phys. Scr. 92 (6) (2017) 065601.
[25] W. Zhang, et al., Nucl. Fusion 60 (12) (2020) 126022.
[26] G. Sun, et al., Phys. Plasmas 22 (9) (2015) 1654.
[27] Jizong Yang, et al., AIP Adv. 10 (2020) 075005.
[28] J. Ma, et al., Nucl. Fusion 57 (2017) 126004.
[29] Z. Lin, et al., Science 281 (1998) 1835.
[30] J. McClenaghan, et al., Phys. Plasmas 21 (2014) 122519.
[31] W. Zhang, et al., Phys. Rev. Lett. 101 (2008) 095001.
[32] I. Holod, et al., Phys. Plasmas 16 (2009) 122307.
[33] J.C. Li, et al., Phys. Plasmas 24 (2017) 082508.
[34] J. Bao, et al., Phys. Plasmas 24 (2017) 102516.
[35] D.J. Liu, et al., Phys. Plasmas 21 (2014) 122520.
[36] H. Cai, et al., Phys. Plasmas 19 (2012) 072506.